

Stability Parameters and Crystal Visualization Studies of Anti-degradable Cobalt Cyclotetraphosphates for Bone Applications

Khaled M. Elsabawy^{a,b,*}, A. El-Maghraby^{b,c}, Waheed F.El-Hawary^{b,d}

^a Materials Science Unit , Chemistry Department ,Faculty of Science,Tanta University-31725-Tanta – Egypt

^b Chemistry Department , Faculty of Science, Taif University, 888- Taif, Kingdom of Saudi Arabia

^c Ceramic Department, Physics Department, National Research Center, Dokki, Tahrir st. ,Egypt

^d Department of Chemistry, Faculty of Science, Cairo University, Giza, Egypt

^{a,b} *khaledelsabawy@yahoo.com ; ksabawy@hotmail.com*

Abstract: *The present investigations concerned by structural parameters specially torsion on angles inside unit cell that responsible for monoclinic lattice. Structural investigations via XRD proved that the monoclinic structure phase with C12/C1 space group and lattice parameter $a = 11.809(2)$, $b = 8.293(1)$, $c = 9.923(2)$ Å respectively is formed with high quality at elevated temperature 1100°C. A visualized investigations were performed to confirm structure validity and stability at temperature of sintering (1100°C) . Visualization studies indicated that variations of bond distances between Co1,Co2,P1 and P2 and different six oxygen atoms (O1 ,O2 , O3 ,O4 ,O5 and O6) inside crystal lattice are responsible for increasing lattice flexibility factor (by controlling in shrinkage and expansion coefficient) and consequently increase its bonds stability to break .*

Keywords: *Stability parameters, Phosphates; Ceramics; XRD; Visualization.*

1. INTRODUCTION

As one of the members of phosphate material family, transition metal cyclotetraphosphate micro-/nanoparticles can be used in potential pigments, selective catalysts, phosphors, materials for corrosion-resistant coatings and biocompatible and biodegradable in tissue [1–8]. Several divalent including 3d metals, namely, Mn, Co, Fe, Zn, Cu, and Ni, are known to form the single metal cyclotetraphosphate $M_2P_4O_{12}$, where M(II) stands for a divalent metal. The binary metal cyclotetraphosphates $M_{2-x}A_xP_4O_{12}$ (M and A=Mg, Ca, Mn, Co, Ni, Zn, or Cu; $x=0-2$), isostructural with the single metal cyclotetraphosphates $M_2P_4O_{12}$, were prepared by Trojan et al. [5–8] and Boonchomet al. [9–11]. All these compounds have similar X-ray diffraction patterns and close unit cell parameters, which crystallize in monoclinic space group C2/c ($Z=4$) [12]. Various methods have been employed to synthesize binary metal cyclotetraphosphates, including two-step thermal method [5–8], hydrothermal synthesis [5] and the decomposition of binary metal (II) dihydrogenphosphates $(M_{1-y}A_y(H_2PO_4)_2 \cdot nH_2O)$; where M and A= Ca, Mg, Mn, Fe, Co, Ni, Cu or Zn; $y=0-1$; $n=1-4$ [9–11]. This work is of interest because it appears economically advantageous to replace partially the divalent metal cations by some cheaper divalent element which could also improve special properties as above mentioned [1–4]. However, it is relevant to synthesize binary cyclotetraphosphate and its solid solution because changing the metal ratio influences its useful properties. Consequently, it is a major challenge to synthesize binary metal cyclotetraphosphate micro-/nanoparticles with its intrinsic shape-dependent properties and resulting application. Recently, cobalt iron pyrophosphate $CoFeP_2O_7$ and cobalt iron cyclotetraphosphate $CoFeP_4O_{12}$ were prepared by mixing of $CoCO_3$, Fe and H_3PO_4 in water–methanol and in water– acetone, respectively [13,14].

The difference of media (solvents) in the precipitation process leads to the obtaining different phosphates, as revealed by XRD and FTIR data. Due to its solubility in water and its ability to associate with metal ions in media, solvent has been used as a binder cum gel for shaping materials (bulk, porous, micro- or nano-particles) and a matrix for entrapment of ions to generate a gelled precursor which resulted in obtaining different material or same material with different size and

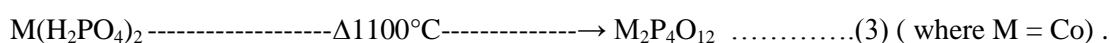
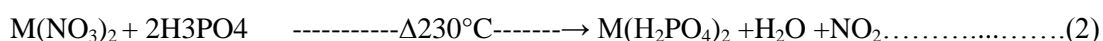
morphology after heat treatment. The results obtained are also in agreement with other phosphate group reported in literature [15,16].

The major goal of the present investigations is understanding the role of structural parameters within crystal lattice of $M_2P_4O_{12}$ that stabilize structure of crystal even at elevated temperatures .

2. EXPERIMENTAL

2.1 Synthesis of Metal-cyclotetraphosphate

The cobalt cyclotetraphosphate was synthesized via three step reactions 1st reaction is dissolving cobalt carbonate in few drops of concentrated nitric acid forming acidic cobalt nitrate then solution neutralized by conc. ammonia solution .2nd step is the reaction with 70% phosphoric acid forming cobalt dihydrogen phosphate at temperature 230°C .3rd step is firing followed by sintering process at 1100°C to form violet powder from pure cobaltcyclotetraphosphate . These steps are in partial agreement with [5] .



The violet powder from pure cobalt cyclotetraphosphate was grounded in agate mortar for 15 min. then the resulted powder forwarded to perform the different structural measurements .

2.2 Structural Measurements

The X-ray diffraction (XRD): Measurements were carried out at room temperature on the fine ground samples using Cu-K α radiation source, Ni-filter and a computerized STOE diffractometer/Germany with two theta step scan technique. Rietveld and indexing of structure were made via Fullprof package and Gsas program.

A visualized studies of crystal structure were made by using Diamond Molecular Structure version 3.2 package, Germany and MERCURY-2.3 depending up on single crystal structural data of pure cobalt cyclotetraphosphates including atomic coordinates of monoclinic phase supplied from ICSD–Karlsruhe-Germany.

A visualization study made is concerned by matching and comparison of experimental and theoretical data of atomic positions, bond distances, oxidation states and bond torsion on the crystal structure formed. Some of these data can be obtained free of charge from The Cambridge Crystallographic Data Centre via www.ccdc.cam.ac.uk/data_request/cif, or by emailing data_request@ccdc.cam.ac.uk, or by contacting ICSD-Fiz-Karlsruhe-Germany.

3. RESULTS AND DISCUSSION

3.1 Structural Identification

Fig.1 displays x-ray diffraction patterns of cobalt cyclotetraphosphate at different sintering temperature 1100°C. The accurate analyses of these patterns were performed by using both of rietveld and indexing via Fullprof package and Gsas program. The analysis is focused on the main intense reflection peaks (Fingerprint of structure) and indicated that cobalt cyclotetraphosphate is mainly belong to single monoclinic phase with $C12/c1$ space group as symbolized by pink cycles in Fig.1 and only very few percentage of cobalt oxide as secondary phase in minor . It was observed that the impurity phases are decreasing as sintering temperatures are increasing as shown in Fig.1 where impurity phases are assigned by blue squares. The comparisons of most intense reflections peaks in all patterns (fingerprint reflections represent monoclinic –phase) indicated that cobalt cyclotetraphosphate which is sintered at 1100°C is the best fit one with high purity than others which sintered at temperatures 600,800 and 1000°C respectively .

In the hypothesis of isostructural, due to existence of cobalt (II) and Cobalt (III) the spectrum peaks for the system of cobalt cyclotetraphosphate (solid solution) which is single metal cyclotetraphosphate ($M_2P_4O_{12}$, $M=Co$) are quite similar because of the equivalent electronic charges and the close radii of cations . Consequently, all the diffraction peaks in the Fig.1 are found to be in agreement with monoclinic $M_2P_4O_{12}$ and space group $C12/c 1$ without violation. Only few characteristic peaks of other impurities (e.g.Co-Oxide) was clearly observed at lower sintering temperatures (600, 800°C).

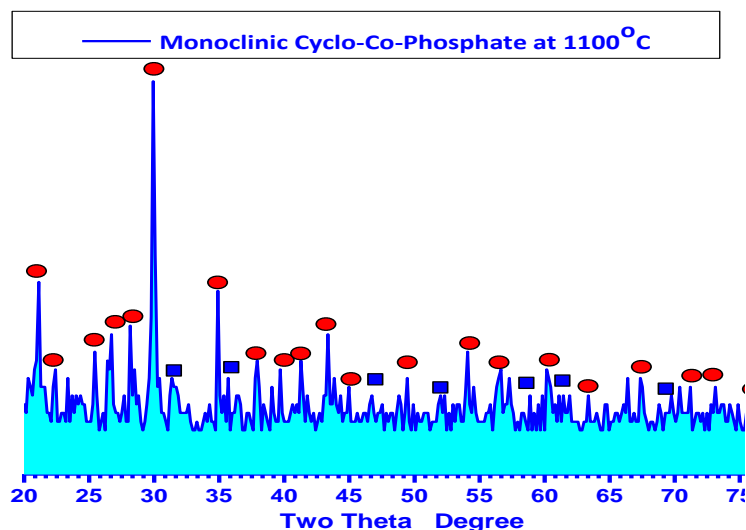
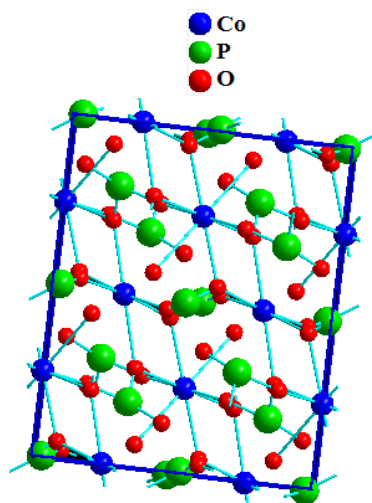


Fig.1. X-ray diffraction patterns of cobalt cyclotetraphosphate at 1100°C sintering temperature

From XRD analysis (Fig. 1), grain size evaluated and calculated according to the Scherrer's formula: $D = K\lambda / (\beta \cos \theta)$, where D is particle diameter, $K=0.89$ (the Scherrer's constant), $\lambda=1.5406$ (wavelength of the X-ray used), β is the width of line at the half-maximum intensity and θ is the corresponding angle. The average crystallite size of product is estimated from the strongest three diffraction peaks below 40° for 2θ and found to be 98 ± 11 nm. This crystallite size of the prepared cobalt cyclotetraphosphate is smaller than those data estimated from SEM and AFM-investigations which confirm that the powder mixture of cobalt cyclotetraphosphate is not unified grain sizes and grain sizes are varied in the bulk than surface's layers. The lattice parameters were calculated from the XRD spectra and found to be $a = 11.809(2)$, $b = 8.293(1)$, $c = 9.923(2)$ Å, which are very close to those of the standard data file (ICSD #300027) and the literatures [9–11,14].

3.2 Stability Parameters Studies

Fig.2 displays the unit cell of cobalt cyclotetraphosphate which built up via DIAMOND IMPACT CRYSTAL PROGRAM version 3.2 depending up on the single crystal data and atomic coordinates locations of pure cobalt cyclotetraphosphate. The unit cell was visualized and built up with minimum 138 atoms = (Co =16 ,P =38 and O = 94 atoms) and four edges. A visualization study made is concerned by matching and comparison of experimental and theoretical data of atomic positions, bond distances, oxidation states and bond torsion on the crystal structure formed.



Co₂P₄O₁₂ Structure with C₁₂/C₁ Space Group and Monoclinic AB₂X₆ Structure Type

Fig.2. Unit cell of monoclinic cobalt cyclotetraphosphate

Many researchers in the last did their best to understand the crystallographic structure of phosphates (open phosphates or cyclic poly phosphates) [20-28].

The initial analysis of structural parameters inside visualized crystal lattice of cobalt cyclotetraphosphate indicated that there are two different types of cobalt namely (Co1 and Co2), Two types of phosphorous atoms (P1 and P2) and finally six different types of oxygen atoms namely (O1,O2,O3,O4,O5 and O6) .

The comparison between visualized XRD-profile Fig.3 and the experimental XRD-pattern sintered at 1100 °C Fig.1 , indicated that there is type of fitting coupled with high figure of merit between both patterns specially on the point of view positions of most intense reflection peaks on both patterns .The shifts on some intense reflection peak position within limits of two theta values ~ 2 degree could due to impurity phases interactions with the main monoclinic structure of cobalt cyclotetraphosphate on the experimental pattern .

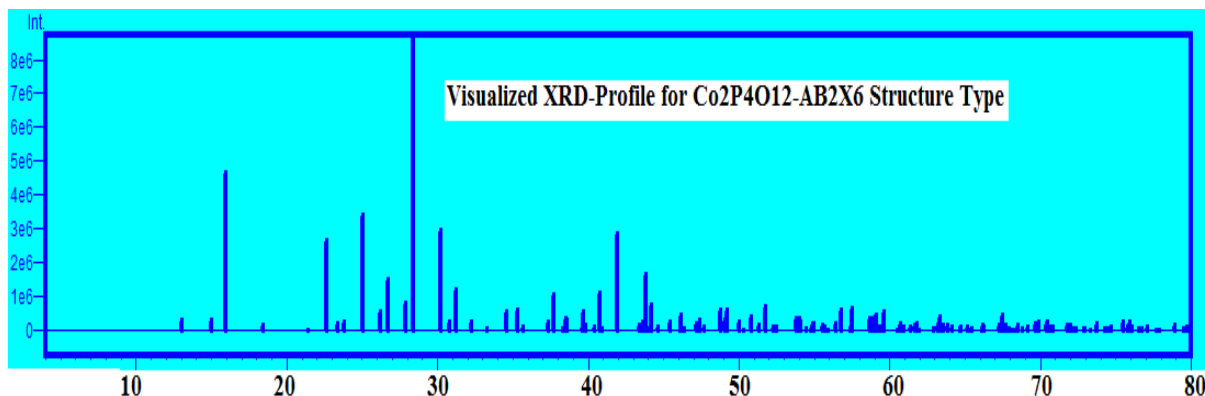


Fig.3. Visualized XRD-profile constructed for monoclinic $Co_2P_4O_{12}$ with $C12/C1$ space group

Fig.4 displays the regular distribution of PO_3 -polyhedra throughout the unit cell of cobalt cyclotetraphosphate .The analysis of these polyhedron indicated that the phosphorous atom as central ion was surrounding by oxygen atoms, three oxygen atoms represents the triangle base lie at ~ nearly the same distance from phosphorous (central metal ion) while the fourth one at distance longer than the others three oxygen of triangle base.

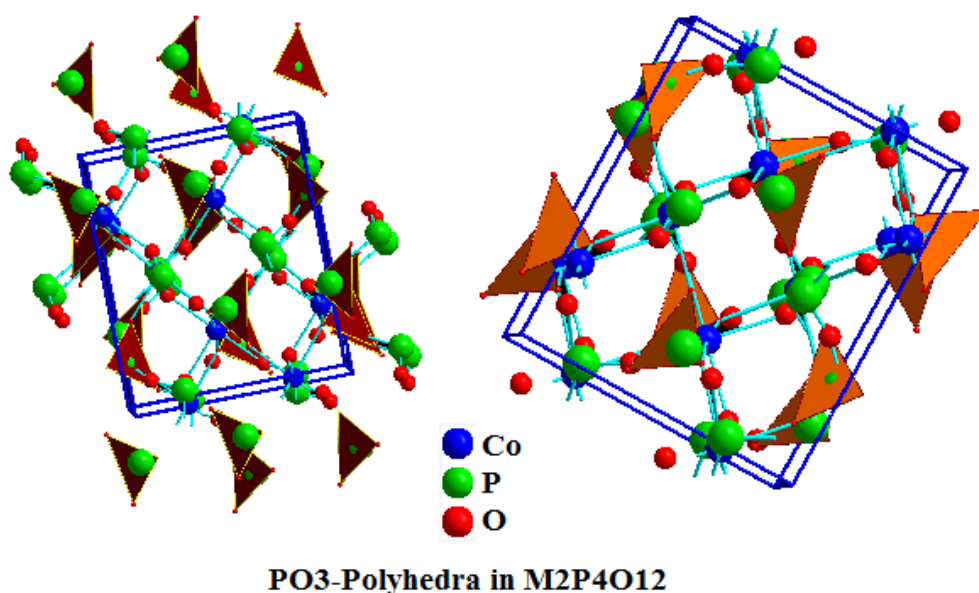


Fig.4. Distribution of PO_3 -polyheral in the unit cell of cobalt cyclotetraphosphate

The accurate analysis of bond lengths, torsion on angles inside the crystal lattice of cobalt cyclotetraphosphate (Tables.1-5) can enhance us understand what is the structural factors responsible for lattice stability .

The analysis of data in Tables .1,2 ,3 one can conclude the following observations;

Stability Parameters and Crystal Visualization Studies of Anti-degradable Cobalt Cyclotetraphosphates for Bone Applications

Table.1. Selected bond lengths and angles inside crystal lattice of $Co_2P_4O_{12}$

Atom1	Atom2	d1-2 Å	Atom3	d1-3 Å	Angle 312^
Co1	O1	2.0927	O1	2.0927	180.000
	O1	2.0927	O2	2.3366	82.238
	O1	2.0927	O2	2.3366	97.762
	O2	2.3366	O2	2.3366	180.000
	O2	2.3366	O5	2.4865	116.323
	O5	2.4865	O3	2.8210	57.061
	O5	2.4865	P1	3.0353	157.072
	O3	2.8210	O3	2.8210	180.000
	O3	2.8210	P2	2.9164	144.014
	P2	2.9164	P2	2.9164	180.000
	P2	2.9164	P1	3.0353	71.568
	P2	2.9164	O4	3.5270	29.627
	P2	2.9164	O6	3.5756	80.753
	P1	3.0353	P1	3.0353	180.000
	P1	3.0353	O6	3.5756	21.363
	O4	3.5270	O6	3.5756	96.488
	O4	3.5270	O6	3.5756	83.512
	O6	3.5756	O6	3.5756	180.000
	O6	3.5756	P2	3.6583	79.758
	O6	3.5756	P2	3.6583	100.242

Table.2. Selected bond lengths and angles inside crystal lattice of $Co_2P_4O_{12}$

Atom1	Atom2	d1-2 Å	Atom3	d1-3 Å	Angle 312^
Co2	O6	2.1694	O6	2.1694	93.593
	O6	2.1694	O5	2.3208	84.836
	O6	2.1694	O5	2.3208	174.602
	O6	2.1694	O2	2.5737	112.127
	O6	2.1694	O2	2.5737	71.914
	O5	2.3208	O4	3.5398	76.791
	O5	2.3208	P2	3.7464	74.787
	O5	2.3208	P2	3.7464	116.925
	O5	2.3208	O3	3.9043	138.211
	O5	2.3208	O3	3.9043	120.351
	O2	2.5737	O2	2.5737	174.457
	O2	2.5737	P1	3.1577	77.031
	O2	2.5737	O6	3.3434	98.404
	O2	2.5737	O6	3.3434	80.635
	P1	3.1577	O4	3.5398	93.099
	P1	3.1577	O3	3.9043	107.617
	P1	3.1577	O3	3.9043	136.556
	O6	3.3434	O6	3.3434	160.281
	O6	3.3434	P1	3.4087	138.822
	O6	3.3434	O1	3.5271	113.415
	P1	3.4087	P1	3.4087	79.006
	P1	3.4087	O1	3.5271	84.012
	P1	3.4087	O1	3.5271	67.309
	P1	3.4087	O4	3.5398	103.558
	O1	3.5271	P2	3.7464	25.747
	O1	3.5271	P2	3.7464	144.026
	O1	3.5271	O3	3.9043	56.224
	O1	3.5271	O3	3.9043	87.439
	O4	3.5398	O4	3.5398	88.346
	O4	3.5398	P2	3.7464	74.116
	O4	3.5398	P2	3.7464	118.697
	P2	3.7464	O3	3.9043	72.236
	P2	3.7464	O3	3.9043	91.882
	P2	3.7464	O3	3.9043	91.882

	P2	3.7464	O3	3.9043	72.236
	O3	3.9043	O3	3.9043	37.949

Table.3. Selected bond lengths and angles inside crystal lattice of $Co_2P_4O_{12}$

Atom1	Atom2	d1-2 Å	Atom3	d1-3 Å	Angle 312 [^]
P1	O5	1.2222	O6	1.3354	112.012
	O5	1.2222	O3	1.8394	111.327
	O5	1.2222	O4	1.9623	98.852
	O5	1.2222	Co1	3.0353	52.425
	O6	1.3354	O1	3.8450	71.883
	O6	1.3354	O6	3.9043	47.653
	O1	3.4635	O1	3.9266	106.380
	O1	3.4635	O2	3.9527	25.309
	O1	3.4635	P1	3.9812	156.181
	O3	1.8394	Co1	3.0353	65.455
	O3	1.8394	Co2	3.1577	148.445
	O4	1.9623	O1	3.9266	47.041
	O4	1.9623	O2	3.9527	87.564
	O4	1.9623	P1	3.9812	64.088
	Co1	3.0353	Co2	3.1577	83.872
	Co1	3.0353	O3	3.3910	107.797
	Co1	3.0353	Co2	3.4087	90.253
	Co2	3.1577	P2	3.4815	133.588
	Co2	3.1577	O1	3.5216	76.412
	O3	3.3910	O1	3.8450	90.375
	Co2	3.4087	O1	3.9266	108.957
	Co2	3.4087	O2	3.9527	40.078
	O2	3.5532	O2	3.9527	62.931
	O2	3.5532	P1	3.9812	152.445
	O3	3.4278	P2	3.4815	82.722
	P2	3.4815	O1	3.5216	59.248
	P2	3.5485	O2	3.5982	110.496
	O4	3.5878	O2	3.5982	95.547
	O4	3.5878	O1	3.8450	84.205
	O4	3.5878	O6	3.9043	96.550
	O4	3.5878	O1	3.9266	72.730

Table.4. Selected bond lengths and angles inside crystal lattice of $Co_2P_4O_{12}$

Atom1	Atom2	d1-2 Å	Atom3	d1-3 Å	Angle 312 [^]
P2	O2	1.3584	O1	1.6346	90.263
	O2	1.3584	O4	1.7500	122.795
	O1	1.6346	O5	3.8101	159.446
	O1	1.6346	O4	3.8181	47.186
	O1	1.6346	O5	3.8547	102.964
	O4	1.7500	O3	1.7746	85.307
	O4	1.7500	Co1	2.9164	94.901
	O3	1.7746	O5	3.8101	34.432
	O3	1.7746	O5	3.8547	105.956
	Co1	2.9164	O5	3.4562	164.249
	Co1	2.9164	O1	3.4618	37.075
	O5	3.4562	O4	3.8181	61.446
	O5	3.4562	O5	3.8547	151.691
	O1	3.4618	P1	3.4815	60.953
	O1	3.4618	P1	3.5485	68.115
	P1	3.5485	O5	3.8101	69.465
	P1	3.5485	O4	3.8181	128.505
	P1	3.5485	O5	3.8547	127.918
	O6	3.5725	O3	3.5777	169.950
	O6	3.5725	Co1	3.6583	84.063
	O3	3.5777	O4	3.8181	51.319

Stability Parameters and Crystal Visualization Studies of Anti-degradable Cobalt Cyclotetraphosphates for Bone Applications

	O3	3.5777	O5	3.8547	130.744
	Co1	3.6583	O2	3.7104	36.966
	Co1	3.6583	O1	3.7128	122.659
	O5	3.6692	O5	3.8547	147.193
	O2	3.7104	O1	3.7128	156.019
	Co2	3.7464	O5	3.8547	35.519
	O5	3.8101	O4	3.8181	112.308

Table.5. Selected bond lengths and angles inside crystal lattice of $Co_2P_4O_{12}$

Atom1	Atom2	d1-2 Å	Atom3	d1-3 Å	Angle 312 [^]
O1	P2	1.6346	Co1	2.0927	157.754
	P2	1.6346	O2	2.1302	39.621
	P2	1.6346	P1	3.9266	82.859
	Co1	2.0927	O2	2.1302	151.780
	Co1	2.0927	O5	2.6771	61.400
	O2	2.1302	O6	3.6570	81.232
	O2	2.1302	P2	3.7128	114.101
	O2	2.9186	O4	2.9451	75.146
	O2	2.9186	O4	2.9609	129.658
	O4	2.9451	O5	3.7359	138.844
	O4	2.9451	O6	3.7769	69.906
	O3	3.0569	O2	3.3406	135.391
	O3	3.0569	P2	3.4618	113.44
	O2	3.3406	P1	3.9266	79.250
	P2	3.4618	O3	3.5075	29.494
	O3	3.5174	O3	3.8471	157.065
	O3	3.5174	P1	3.9266	159.635
	P1	3.5216	Co2	3.5271	163.460
	P1	3.5216	O6	3.6570	129.656
	Co2	3.5271	P1	3.9266	118.457
	O6	3.6570	P2	3.7128	70.152
	P2	3.7128	P1	3.9266	148.032
	O5	3.7359	O6	3.7769	79.868
	O5	3.7359	P1	3.8450	18.483
	O5	3.7359	O3	3.8471	140.930
	O5	3.7359	P1	3.9266	120.490
	O6	3.7769	O3	3.8471	138.211
	O6	3.7769	P1	3.9266	141.255
	P1	3.8450	O3	3.8471	159.386
	O3	3.8471	P1	3.9266	27.350

Cobalt type one symbolized as (Co1) was linked with all types of oxygen atoms recording the following bond lengths (2.0927 , 2.3366 , 2.8210 , 3.5270 , 2.4865 and 3.5756 Å) corresponding to Co1-O1 , Co1-O2 , Co1-O3 , Co1-O4 , Co1-O5 and Co1-O6 bond lengths respectively .From these notifications one can conclude that O1,O2 and O3 could be located as triangle base of PO_3^- while O4,O5 and O6 can be oriented as axial oxygen to complete the vacant site of tetrahedron forming PO_4^- anion.

The cobalt type one (Co1) also is linked with two different types of phosphorous namely (P1 and P2) with bond distances 3.0353 and 2.9164 Å respectively which confirm that cobalt has more than one oxidation state over the original common oxidation (CoII and CoIII) inside crystal lattice of cobalt cyclotetraphosphates . Thus could lead to informative scientific knowledge that oxidation state of cobalt takes values between Co^{2+} , Co^{m+} , Co^{3+} (where m fractions between 2 ,3 and $2 \leq m \leq 3$). This result can interpret why the bond lengths of cobalt with six oxygen atoms are different. Plus effect of coupling of charges due to environmental neighboring groups.

Cobalt type two (Co2) has similar behavior to cobalt type one but the oxygen atoms that represent triangle base are recommended to be O2,O5 and O6 with bond lengths 2.5737 ,2.3208 and 2.1694 Å respectively while axial oxygen atoms could be occupied by O1,O3 and O4 with bond distances 3.5271 ,3.9043 and 3.5398 Å respectively .

The cobalt type two (Co2) is also linked with the two different types of phosphorous atoms namely (P1 and P2) with bond distances 3.1577 and 3.7464 Å which confirm that cobalt has more than one oxidation state within the crystal lattice . Similar behavior of existence multi oxidation states was reported in references [20,21] in which the conditions of synthesis at elevated temperatures in air or oxygen were responsible .

With respect to phosphorous atoms (P1 and P2) it were observed that phosphorous type one (P1) was linked inside crystal lattice with all oxygen atoms recording bond lengths 1.2222 ,1.3334 and 1.9623 Å correspond to P1-O5 ,P1-O6 and P1-O4 respectively these bond distances are suitable to be base triangle of PO₃⁻ while the rest three oxygen atoms O1 ,O2 and O3 recorded bond distances 3.4635 ,3.5532 and 3.3910 which are suited to be axial atoms .

In conclusion , one can conclude that variations of bond distances between Co1,Co2,P1 and P2 and different six oxygen atoms (O1 ,O2 , O3 ,O4 ,O5 and O6) inside crystal lattice are responsible for increasing lattice flexibility factor (by controlling in shrinkage and expansion coefficient) and consequently increase its bonds stability to break . These facts can be attributed to three main factors inside lattice 1st oxidation state of cobalt takes values between Co²⁺ ,Co^{m+} ,Co³⁺ (where m fractions between 2 ,3 and 2 ≤ m ≤ 3). 2nd effect of coupling of charges due to environmental neighboring groups effects .3rd the six oxygen atoms are liable to replace each other throughout the lattice to compensate any lattice defects could break bonds (evidence is exchanging positions of triangle base with axial positions) .

REFERENCES

- [1]. Jouini, A.; Gacon, J. C.; Ferid, M.; Trabelsi-Ayadi, M. Optical properties of praseodymium concentrated phosphates. *Opt. Mater.* 2003,24, p.175.
- [2]. Kitsugi, T.; Yamamuro, T.; Nakamura, T.; Oka, M. Transmission electron microscopy observations at the interface of bone and four types of calcium phosphate ceramics with different calcium/phosphorus molar ratios. *Biomaterials* 1995, 16, p.1101.
- [3]. Jian-Jiang, B.; Dong-Wan, K.; Kug Sun, H. Microwave dielectric properties of Ca₂P₂O₇. *J. Eur. Ceram. Soc.* 2003, 23, p.2589.
- [4]. Martinelli, J. R.; Sene, F. F.; Gomes, L. Synthesis and properties of niobium barium phosphate glasses. *J. Non-Cryst. Solids* 2000, 263, p.299.
- [5]. Parada, C.; Perles, J.; Saez-Puche, R.; Ruiz-Valero, C.; Snejko, N. Crystal growth, structure, and magnetic properties of a new polymorph of Fe₂P₂O₇. *Chem. Mater.* 2003, 15, p.3347.
- [6]. Antraptseva, N. M.; Shchegrov, L. N.; Ponomareva, I. G. Thermolysis features of Manganese (II) and zinc dihydrogenphosphate solid solution. *Russ. J. Inorg. Chem.* 2006, 51,p. 1493.
- [7]. Trojan, M.; Brandova, D. A study of thermal preparation of c-Mn₂P₄O₁₂. *J. Therm. Anal. Calorim.* 1985, 30, p.159.
- [8]. Trojan, M. Double tetrametaphosphates Mn_{2-x}Ca_xP₄O₁₂ as special pigments. *Dyes Pigm.* 1990, 12, p.35.
- [9]. Trojan, M. Binary cyclotetraphosphates Zn_{2-x}Ca_xP₄O₁₂ as new special pigments. *Dyes Pigm.* 1990, 13,p. 1.
- [10].Trojan, M.; Sýulcova, P.; Mosner, P. The synthesis of binary zinc-(II)-nickel(II)cyclotetraphosphates as new special pigments. *Dyes Pigm.* 2000, 44, p.161.
- [11].Trojan, M. A study of the reactions during formation of c-Ni₂P₄O₁₂. *Thermochim. Acta* 1990, 160,p. 361.
- [12].Trojan, M.; Brandova, D. A study of the thermal preparation of c-Cd_{4/3}Ca_{2/3}P₄O₁₂. *Thermochim. Acta* 1990, 160, p.349.
- [13].Trojan, M.; Sýulcova, P. Binary Cu(II)-Mn(II) cyclo-tetraphosphates. *Dyes Pigm.* 2000, 47, p.291.
- [14].Trojan, M.; Brandova, D.; Paulik, F.; Arnold. M. Mechanism of the thermal dehydration of Co_{1/2}Ca_{1/2}(H₂PO₄)₂·2H₂O. *J. Therm. Anal. Calorim.* 1990, 36, p.929.
- [15].Trojan, M.; Brandova, D. Mechanism of dehydration of Zn_{0.5}- Mg_{0.5}(H₂PO₄)₂·2H₂O. *Thermochim. Acta* 1990, 159, p.1.

- [16]. Brandova, D.; Trojan, M.; Arnold, M.; Paulik, F. Thermal study of decomposition of $\text{Cu}_1/2\text{Mg}_1/2(\text{H}_2\text{PO}_4)_2 \cdot 0.5 \text{H}_2\text{O}$. *J. Therm. Anal. Calorim.* 1990, 36, p. 677.
- [17]. V. Ramakrishnan, G. Aruldas, Vibrational spectra of Cu(II) and Co(II) tetrametaphosphates, *Infrared Phys.* 25 (1985) pp. 665–670.
- [18]. E.J. Baran, R.C. Mercader, A. Massafiero, E. Kremer, Vibrational and ^{57}Fe -Mössbauer spectra of some mixed cation diphosphates of the type $\text{MIIIFe}_2\text{III}(\text{P}_2\text{O}_7)_2$, *Spectrochim. Acta.* 60 (2004) pp. 1001–1005.
- [19]. E.H. Soumhi, I. Saadoune, A. Driss, A new organic-cation cyclotetraphosphate $\text{C}_{10}\text{H}_{28}\text{N}_4\text{P}_4\text{O}_{12} \cdot 4\text{H}_2\text{O}$: crystal structure, thermal analysis, and vibrational spectra, *J. Solid State Chem.* 156 (2001) pp. 364–369.
- [20]. Averbuch-Pouchot, M. T., Durif, A.: Crystal structure of lead tetrapolyphosphate: $\text{Pb}_3\text{P}_4\text{O}_{13}$. *Acta Crystallogr.* C43 (1987) pp. 631-632.
- [21]. Chudinova, N. N., Lavrov, A. V., Tananaev, I. V.: Reaction of bismuth oxide with phosphoric acid during heating. *Izv. Akad. Nauk SSSR, Neorg. Mater.* 8 (1972) pp. 1971-1976.
- [22]. Durif, A., Averbuch-Pouchot, M. T., Guitel, J. c.: Structure cristalline de $(\text{NH}_4)_3\text{SiP}_4\text{O}_{13}$: un nouvel exemple de silicium hexacoordine. *Acta Crystallogr.* B32 (1976) pp. 2957 - 2960.
- [23]. Enraf-Nonius: Structure Determination Package. RSX 11M version. Enraf-Nonius, Delft (1977).
- [24]. Hilmer, N., Chudinova, N. N., Jost, K. H.: Condensed bismuth phosphates. *Izv. Akad. Nauk SSSR, Neorg. Mat.* 14 (1978) pp. 1507-1515.
- [25]. *International Tables for X-ray Crystallography* (Present distributor D. Reidel, Dordrecht), Vol. IV, Birmingham: Kynoch Press (1974).
- [26]. Palkina, K., Jost, K. H.: Crystal structure of the polyphosphate $\text{BiH}_3\text{P}_3\text{O}_{10}$. *Acta Crystallogr.* 831 (1975) pp. 2285 - 2290.
- [27]. Schulz, I.: Über zwei kristalline Tetraphosphate. *Z. Anorg. Allg. Chem.* 287 (1956) pp. 106-112.
- [28]. Tezikova, L. A., Chudinova, N. N., Fedorov, P. M., Lavrov, A. V.: Bismuth acid pyrophosphate. *Izv. Akad. Nauk SSSR, Neorg. Mat.* 10 (1974) pp. 2057 -2063.
- [29]. Khaled M. Elsabawy, Nader H. Elbagoury, Structure Visualization and AFM-Surface Microstructural Investigations on Ni-Ti-O Mixed Oxide With ABX_3 -Structure of Cast Ni-Superalloy, *Adv. Appl. Science. Res.* 2,2(2011) pp. 38-47.
- [30]. Khaled M. Elsabawy, Structure Visualization, Mechanical Strength Promotion and Raman Spectra of Hafnium Doped -123-YBCO Superconductor synthesized via Urea Precursor Route, *Cryogenics* 51(2011) pp. 452-459.

AUTHORS' BIOGRAPHY



Prof. Dr. Khaled M. Elsabawy, (Professor of Materials Sciences – Faculty of Science-Tanta University-Egypt), Executive Editor Der Chemica Sinica Journal, Regional Editor Science Alerts –USA.



Prof. Dr. Ahmed El-Maghraby, (Professor of Ceramics Materials – National Institute of Research-Egypt).



Prof. Dr. Waheed F. El-Hawary, (Associated Professor of Analytical Chemistry- Cairo University-Egypt)